



EUROPEAN
HEMATOLOGY
ASSOCIATION



Ferrata Storti
Foundation

Haematologica 2018
Volume 103(10):1730-1740

Cytoprotective and pro-angiogenic functions of thrombomodulin are preserved in the C loop of the fifth epidermal growth factor-like domain

Xiangmin Wang,^{1,2} Bin Pan,^{1,2} Goichi Honda,³ Xintao Wang,² Yuko Hashimoto,⁴ Hiroshi Ohkawara,² Kailin Xu,¹ Lingyu Zeng¹ and Takayuki Ikezoe²

¹Department of Hematology, The Affiliated Hospital of Xuzhou Medical University, Xuzhou, China; ²Department of Hematology, Fukushima Medical University, Japan; ³Medical Affairs Department, Asahi Kasei Pharma, Kanda Jinbocho, Chiyoda-ku, Tokyo, Japan and ⁴Department of Diagnostic Pathology, Fukushima Medical University, Japan

ABSTRACT

We previously found that the fifth epidermal growth factor-like domain of thrombomodulin (TME5) exerts cytoprotective and pro-angiogenic functions *via* G-protein coupled receptor 15 (GPR15). TME5 is comprised of three S-S bonds that divide it into three loops: A (TME5A), B (TME5B), and C (TME5C). Herein we identified the minimum structure of TME5 that produces favorable effects in vascular endothelial cells (ECs). We found that TME5C, composed of 19 amino acids, but not TME5A or TME5B, stimulated the proliferation of human umbilical vein endothelial cells (HUVECs) and human hepatic sinusoidal endothelial cells (HHSECs). Matrigel plug assays showed that TME5C stimulates *in vivo* angiogenesis. In addition, TME5C counteracted calcineurin inhibitor-induced apoptosis and vascular permeability in HUVECs and HHSECs. Western blot analysis indicated that exposure of either HUVECs or HHSECs to TME5C increased the levels of anti-apoptotic myeloid cell leukemia-1 protein in association with the activation of signal transduction pathways, including extracellular signal-regulated kinase, AKT, and mitogen-activated protein kinase p38. Importantly, TME5C did not affect the coagulation pathway *in vitro*. The cytoprotective function of TME5C was mediated by cell surface-expressed GPR15, as TME5C was not able to protect vascular ECs isolated from *Gpr15* knock-out (KO) mice. Strikingly, TME5C successfully ameliorated sinusoidal obstruction syndrome in a murine model by counteracting the reduction of sinusoidal EC numbers. Taken together, the cytoprotective and pro-angiogenic functions of TM are preserved in TME5C. The use of TME5C may be a promising treatment strategy to prevent or treat lethal complications, such as sinusoidal obstruction syndrome, whose pathogenesis is based on endothelial insults.

Correspondence:

ikezoet@fmu.ac.jp or zengly2000@163.com

Received: December 18, 2017.

Accepted: June 13, 2018.

Pre-published: June 14, 2018.

doi:10.3324/haematol.2017.184481

Check the online version for the most updated information on this article, online supplements, and information on authorship & disclosures: www.haematologica.org/content/103/10/1730

©2018 Ferrata Storti Foundation

Material published in *Haematologica* is covered by copyright. All rights are reserved to the Ferrata Storti Foundation. Use of published material is allowed under the following terms and conditions:

<https://creativecommons.org/licenses/by-nc/4.0/legalcode>.

Copies of published material are allowed for personal or internal use. Sharing published material for non-commercial purposes is subject to the following conditions:

<https://creativecommons.org/licenses/by-nc/4.0/legalcode>,

sect. 3. Reproducing and sharing published material for commercial purposes is not allowed without permission in writing from the publisher.



Introduction

Hepatic sinusoidal obstruction syndrome (SOS) is a potentially life-threatening complication after hematopoietic stem cell transplantation (HSCT).¹ The incidence of SOS ranges from 5% to 60%, depending on the conditioning regimen and transplantation type.² The clinical manifestation of SOS includes rapid and unexplained weight gain, ascites, painful hepatomegaly, and jaundice.³ The development of SOS after HSCT is associated with injury to sinusoidal endothelial cells (ECs) and hepatocytes *via* a variety of factors, including a hepatotoxic conditioning regimen, immunosuppressive treatments with calcineurin inhibitors, and lipopolysaccharide (LPS) released by gram-negative bacteria.^{4,5} Due to the paucity of glutathione content in zone III of the liver, sinusoidal ECs are more vulnerable to toxic agents than hepatocytes.⁵ SOS is now referred to as an endothelial syndrome together with transplant-associated thrombotic microangiopathy (TA-TMA) and engraftment syndrome (ES).^{2,6} As a result of endothelial injury, a hypercoagulable state is caused in patients with ES.⁷ As of

yet, clinical trials evaluating the efficacy of anticoagulants or thrombolytics for treatment of endothelial syndrome have not been conducted.⁸⁻¹⁰

Since 2008, recombinant human soluble thrombomodulin (rTM) has been used to treat disseminated intravascular coagulation in Japan. rTM binds thrombin and converts protein C to activated protein C (APC), which inhibits activated factor V and VIII and acts as an anticoagulant.¹¹⁻¹⁴ APC is well known to protect various cell types, including endothelial cells and podocytes, *via* protease-activated receptor 1 and endothelial protein C receptor.¹⁵ rTM counteracted capillary leakage in a patient who developed ES after HSCT.¹⁶ In addition, rTM rescues individuals with SOS and TA-TMA developed after HSCT.¹⁷⁻²¹ We previously showed that rTM possesses the ability to protect vascular ECs in an APC-dependent and ABC-independent manner from various insults, including the calcineurin inhibitor cyclosporine.^{22,23} In addition, we found that the cytoprotective and pro-angiogenic functions of rTM are localized in the fifth epidermal growth factor-like domain of thrombomodulin (TME5), which does not possess the ability to produce APC, although it retains some binding capacity towards thrombin.²⁴ Furthermore, we found that G protein-coupled receptor 15 (GPR15) expressed on vascular ECs is indispensable for the cytoprotective functions of TME5.^{25,26}

TME5 consists of 40 amino acids, including six cysteine residues that form three disulfide bonds, making TME5 a structure with three separate disulfide-bonded loops: the A loop (residues C390 to C395), B loop (residues C399 to C407), and C loop (residues C409 to C421).²⁷ In contrast with the A and B loops, the structure of the C-loop is similar to that of epidermal growth factor (EGF).²⁷ In the study herein, we identified the minimum structure of TME5 that exerts its cytoprotective and pro-angiogenic activities *in vitro* and *in vivo*.

Methods

Cell culture

HUVECs were purchased from Lonza Walkersville Inc. (Walkersville, MD, USA) and cultured in endothelial cell growth basal medium-2 (EBM-2) culture medium supplemented with endothelial cell growth factors (EGM-2; Lonza Walkersville Inc.). Human hepatic sinusoidal endothelial cells (HHSECs) were purchased from ScienCell (San Diego, CA, USA) and cultured (37°C, 5% CO₂) in endothelial cell medium (ECM, containing 5% fetal bovine serum (FBS; ScienCell).

Murine thoracic aorta vascular ECs were isolated from mice as previously described.²⁸ Briefly, mice were anesthetized, and the thoraces were opened to expose the heart and lungs. The aorta was dissected out and immersed in 20% FBS dulbecco's modified eagle medium (FBS-DMEM; Wako, Tokyo, Japan) in the presence of collagenase type II (Sigma-Aldrich, Tokyo, Japan) for 45 min at 37°C. The cells were then collected and cultured with DMEM supplemented with endothelial cell growth supplement (Sigma-Aldrich, Tokyo, Japan). Five days later, the cells were harvested and utilized for further experiments.

Mice

Gpr15 knockout (*Gpr15* KO) mice (129/SvEv; 129P2-*Gpr15* tm1.1Litt/J, stock number 008769) were purchased from Jackson Laboratory (Bar Harbor, ME, USA). This strain had been backcrossed to C57BL/6 for three generations before being

Table 1. Amino acid sequences of TME5A, TME5B, and TME5C.

Name	Amino acid sequence
TME5A	QMFCNQACPA
TME5B	DCDPNTQASCE
TME5C	ECPEGYILDDGFICTDIDE
TME5C mutant	ECPEAYILDDGFICTDIDE

TM: thrombomodulin.

used for experiments. Female C57BL/6 mice (8-week-old) were purchased from Japan SLC, Inc. (Hamamatsu, Japan). Female BALB/c (H-2K^d, donor) and female C57BL/6 (H-2K^b, recipient) mice, aged ten weeks and weighing 20-25 g, were purchased from Japan SLC, Inc. All procedures were performed according to the animal care guidelines of Fukushima Medical University. During invasive operations, animals were anesthetized by inhaling isoflurane.

Reagents

TM mutants TME5A (residues C387-C397), TME5B (residues C398-C408), and TME5C (residues C408-C426) were synthesized by the Peptide Institute Inc. (Osaka, Japan). The TME5C mutant with a single amino acid substitution was synthesized by GL Biochem (Shanghai, China). The amino acid sequences are listed in Table 1. Cyclophosphamide (CY) was purchased from Shionogi & Co., Ltd (Osaka, Japan). Busulfan (BU) and tacrolimus (FK506) were purchased from Sigma-Aldrich, Tokyo, Japan. TME5 and rTM were provided by Asahi Kasei Pharma (Tokyo, Japan).

Proliferation assays

HUVECs (5×10⁵ cells/well), HHSECs (5×10⁵ cells/well), or murine ECs (5×10⁵ cells/well) were cultured in 96-well plates containing TME5C (25, 50, 250, 500, 1000 nM), TME5A (500 nM), TME5B (500 nM), or TME5 (30 nM) with or without FK506 (10 µg/ml) for 24 h. Bromodeoxyuridine (BrdU, 10 µM/well) was added and incubated for an additional 4 h. The quantity of BrdU incorporated into cells was assessed in accordance with the manufacturer's protocol (Roche, Basel, Switzerland).

Vascular permeability assay

The effects of FK506 and TM mutants on vascular permeability were measured by a vascular permeability assay kit (Millipore, Billerica, MA). Briefly, HUVECs were plated onto collagen-coated inserts and cultured for 72 h until confluence. After starvation for 24 h, cells were treated with TME5A/B/C (500 nM) or TME5 (30 nM) with or without FK506 (10 µg/ml) for 12 h. Then fluorescein isothiocyanate-dextran was added. The extent of permeability was determined by measuring the fluorescence of the plate well solution (excitation: 485 nm, emission: 535 nm).

In vitro vascular tube formation assay

To evaluate the pro-angiogenic effects of TME5C, TME5A, and TME5B *in vitro*, HUVECs or HHSECs were plated on growth factor-reduced matrigel (Corning corporation, NY, USA) pre-coated 24-well plates (2.0×10⁴ cells/well) and incubated with control diluent, TME5 (30 nM), TME5A/B/C (500 nM), or vascular endothelial growth factor (VEGF; 0.5 nM, positive control). After 8 h, the endothelial cell-derived tube-like structure was photographed using an inverted microscope (KEYENCE BZ-X700, Osaka, Japan) (magnification ×40). The tube length in three randomly chosen fields from each well was measured using NIH ImageJ software (NIH, Bethesda, MA, USA).

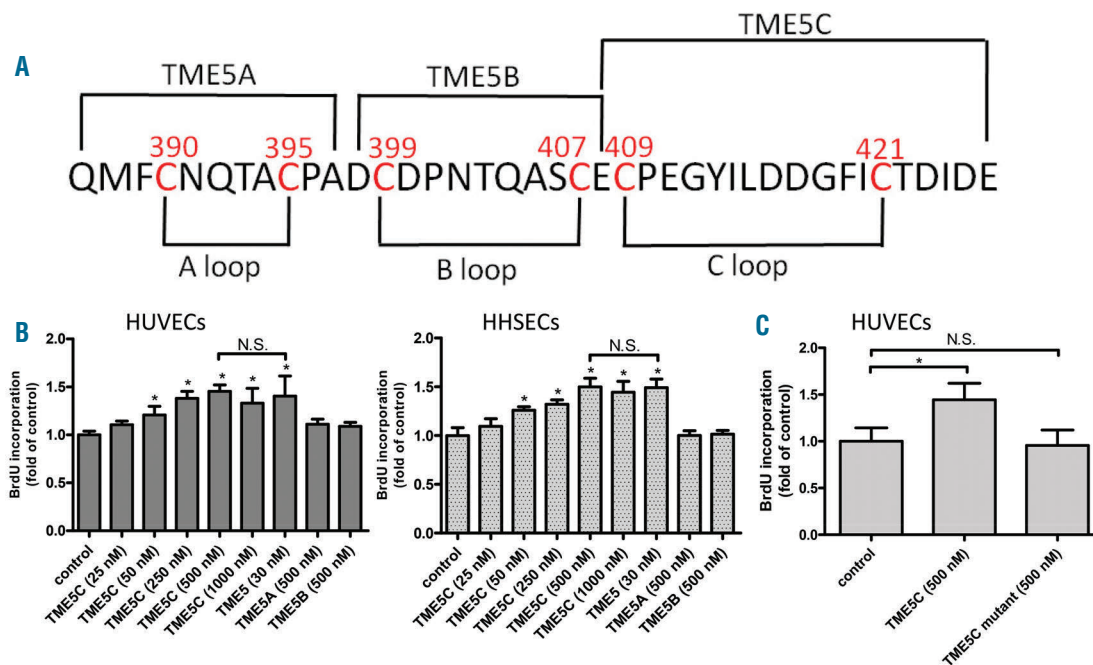


Figure 1. TME5C stimulates proliferation of endothelial cells. (A). Amino acid sequence alignment of TME5A, TME5B, and TME5C. (B, C). BrdU incorporation assay. HUVECs or HHSECs were cultured with TME5C (25, 50, 250, 500, 1000 nM), TME5A (500 nM), TME5B (500 nM), TME5C mutant (500 nM), or TME5 (30 nM) for 24 h. Proliferation was measured by BrdU incorporation assays. Experiments were performed three times in triplicate plates. Results represent the mean \pm SD. * $P < 0.05$. BrdU: bromodeoxyuridine; HUVECs: human umbilical vein endothelial cells; HHSECs: human hepatic sinusoidal endothelial cells; TM: thrombomodulin; N.S.: not significant.

Murine angiogenesis assay

To assess the pro-angiogenic effects of TM mutants *in vivo*, growth factor-reduced matrigel (0.3 mL, containing 40 U/mL heparin) with control diluent, TME5A/B/C (500 nM), TME5 (30 nM), VEGF (0.5 nM, positive control) was subcutaneously injected into C57BL/6 mice (8-week-old, female) near the abdominal midline. Four days later, mice were euthanized, and the matrigel plugs were dissected out and photographed.

Hemoglobin determination of matrigel plugs

Matrigel plugs were mixed with 1 ml distilled water and put on ice for 5–10 min. After centrifugation for 6 min at 8000 g, the supernatants were mixed with drabkin's reagent (Sigma-Aldrich, Tokyo, Japan) and hemoglobin was measured as previously described.²⁴ Absorbance was measured with a microplate reader at 540 nm. Methemoglobin (Sigma-Aldrich, Tokyo, Japan) was used to obtain a standard curve.

Apoptosis Assays

The ability of TM mutants to rescue HUVECs, HHSECs, or murine ECs from FK506-induced apoptosis was measured using the Annexin V Apoptosis Detection Kit (K129, BioVision, Milpitas, CA, USA) and propidium iodide (PI) as previously described.²² Briefly, cells were exposed to FK506 (10 μ g/ml) with or without TME5A/B/C (500 nM) or TME5 (30 nM). After 36 h, cells were harvested and subjected to PI and PE-Cy5 anti-annexin V. Early apoptosis cells are annexin V positive and PI negative. Late apoptosis cells are annexin V positive and PI positive.

Western blot analysis

Western blot analysis was performed as described previously.²² The following antibodies were used: anti-p-ERK (T202/Y204) (Cell Signaling Technology, Danvers, MA, USA),

anti-ERK (Cell Signaling Technology; 9102), anti-p-AKT (Ser473) (Cell Signaling Technology; 9271), anti-AKT (Cell Signaling Technology; 9272), anti-p-Stat5 (Tyr694) (Cell Signaling Technology; 9351), anti-Stat5 (Cell Signaling Technology; 9363), anti-p38 (Cell Signaling Technology; 9212), anti-p-p38 (Tyr180/182) (Cell Signaling Technology; 9216), anti-Mcl-1 (Cell Signaling Technology; 4572), and anti-GAPDH (Cell Signaling Technology; 5174).

Prothrombin time (PT) and activated partial thromboplastin time (APTT)

For PT detection, 200 μ l PT reagent (Sysmex Corporation, Kobe, Japan) was mixed with 100 μ l human plasma with or without rTM, TME5, TME5A/B/C, or TME5C mutant (10 μ l). For APTT detection, 100 μ l APTT reagent (Sysmex Corporation) was mixed with 100 μ l human plasma with or without rTM, TME5, TME5A/B/C, or TME5C mutant (10 μ l). After incubation for 120 s, 100 μ l CaCl_2 was added to this mixture. The clotting time was measured using a KC1 Delta coagulometer (Tcoag, Co. Wicklow, Ireland).

SOS murine model

C57BL/6 mice were randomly divided into three groups ($n=16$ in each group): mice that received vehicle phosphate buffered saline (PBS) without bone marrow transplantation (BMT) were defined as the control group. Mice that received BU/CY followed by BMT and treated with vehicle PBS were defined as the BMT group. Mice that received BU/CY followed by BMT and treated with TME5C were defined as the BMT treated with TME5C group. SOS was induced by previously reported BU/CY reconditioning treatment followed by BMT with some modification;²⁹ in brief, BU (25 mg/kg/day for 4 days) followed by CY (100 mg/kg/day for 2 days) were given to

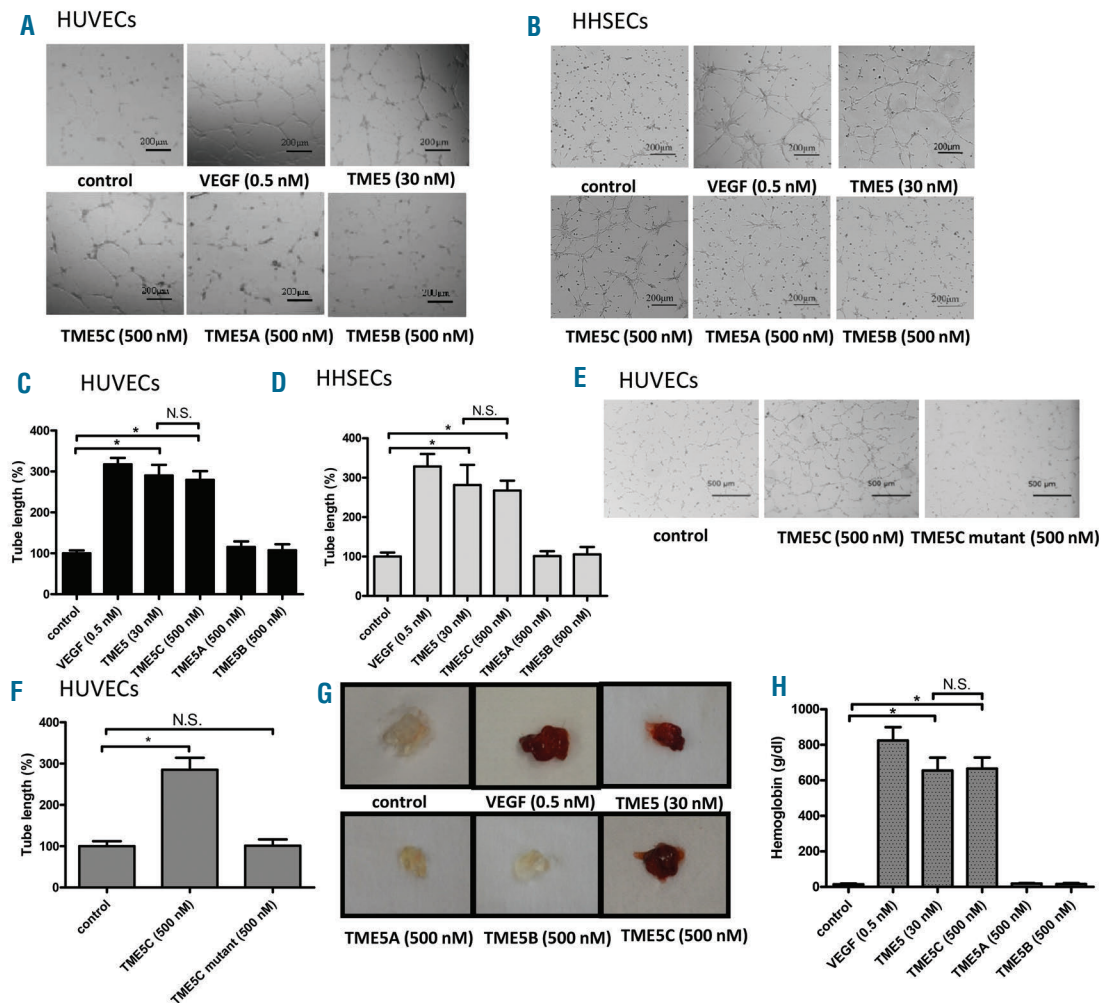


Figure 2. TME5C stimulates angiogenesis in endothelial cells. (A, B, E). *In vitro* vascular tube formation assays. HUVECs or HHSECs were plated on growth factor-reduced matrigel-precoated 24-well plates (2.0×10^4 cells/well) and incubated with control diluent, TME5 (30 nM), TME5A/B/C (500 nM), TME5C mutant (500 nM) or VEGF (0.5 nM, positive control). After 8 h, the endothelial cell-derived tube-like structure was photographed. (C, D, F). The tube length in three randomly chosen fields from each well was measured using NIH ImageJ software. (G, H). *In vivo* angiogenesis assays. Growth factor-reduced matrigel (0.3 ml, containing 40 U/ml heparin) with control diluent, TME5 (30 nM), TME5A/B/C (500 nM), or VEGF (0.5 nM, positive control) was subcutaneously injected into C57BL/6 mice near the abdominal midline ($n=3$ in each group). Four days later, mice were euthanized, and the matrigel plugs were dissected out and photographed. The matrigel plugs were homogenized in the presence of 1 ml distilled water and mixed with drabkin's reagent. The hemoglobin levels were then measured using a microplate reader. Results represent the mean \pm SD. * $P < 0.05$. VEGF: vascular endothelial growth factor; HUVECs: human umbilical vein endothelial cells; HHSECs: human hepatic sinusoidal endothelial cells; TM: thrombomodulin; N.S.: not significant.

the mice intraperitoneally from day -7 to day -4 and from day -3 to day -2, respectively. Two days later, the mice were intravenously infused with bone marrow cells harvested from BALB/C mice (5×10^6 per mouse). The day of BMT was set as day 0. Intraperitoneal administration of either TME5C (500 μ g/kg) or vehicle PBS was initiated on day -7 and continued to day 13. Each agent was given to mice every other day. Blood was withdrawn, and plasma levels of aspartate aminotransferase (AST) and alanine aminotransferase (ALT) were measured on days 7, 14, and 20.

Hematoxylin-eosin (H&E), immunohistochemistry (IHC), and Masson staining

On days 7, 14, and 20 after BMT, some of the mice were sacrificed. Livers were surgically removed and fixed with formaldehyde solution. Specimens were dehydrated, waxed, and sliced into 4- μ m thickness by an RM2126 microtome. After H&E staining, pathologic changes were evaluated under a light micro-

scope. Some liver slices were treated with 3% H_2O_2 and blocked with 1% bovine serum albumin (BSA). The slices were then incubated with primary pan-endothelial cell monoclonal antibody (MECA-32, Novus Biologicals, Littleton, MA, USA) followed by incubation with biotinylated goat anti-rat secondary antibody and ABC HRP reagent. Color was developed with 3,3'-diaminobenzidine. Quantification of MECA-32-positive stained sinusoidal ECs was performed using NIH ImageJ software and expressed as the number of positive stained cells/analyzed area. Masson staining was carried out in accordance with the manufacturer's protocol (Sigma-Aldrich, Tokyo, Japan).

SOS score

Histological slices after H&E, IHC, or Masson staining were blindly evaluated according to the scoring system modified from that described by DeLeve *et al.*³⁰ Based on the total score, the observed SOS was ranked as mild, moderate, or severe as previously described.³¹

TUNEL staining

Apoptosis of hepatocytes and sinusoidal ECs was assessed using an *in situ* cell death detection kit (Roche) according to the manufacturer's protocol. Briefly, paraffin-embedded liver tissue sections were pretreated with dewaxation, rehydration, and proteinase K working solution, and subsequently the terminal deoxynucleotidyl transferase-mediated dUTP nick-end labeling (TUNEL) reaction mixture was added before adding the convert-POD. After the substrate solution was added, the slides were evaluated under a light microscope ($\times 400$).

ELISA

The plasma of mice was collected and analyzed with an enzyme-linked immunosorbent assay (ELISA) kit to measure the concentrations of TM, fibrinogen/fibrin degradation product (FDP), and plasminogen activator inhibitor-1 (PAI-1) according to the manufacturer's protocol (Cloud-Clone Corp. Wuhan, China).

Statistical analysis

Statistical analyses were performed to assess the differences

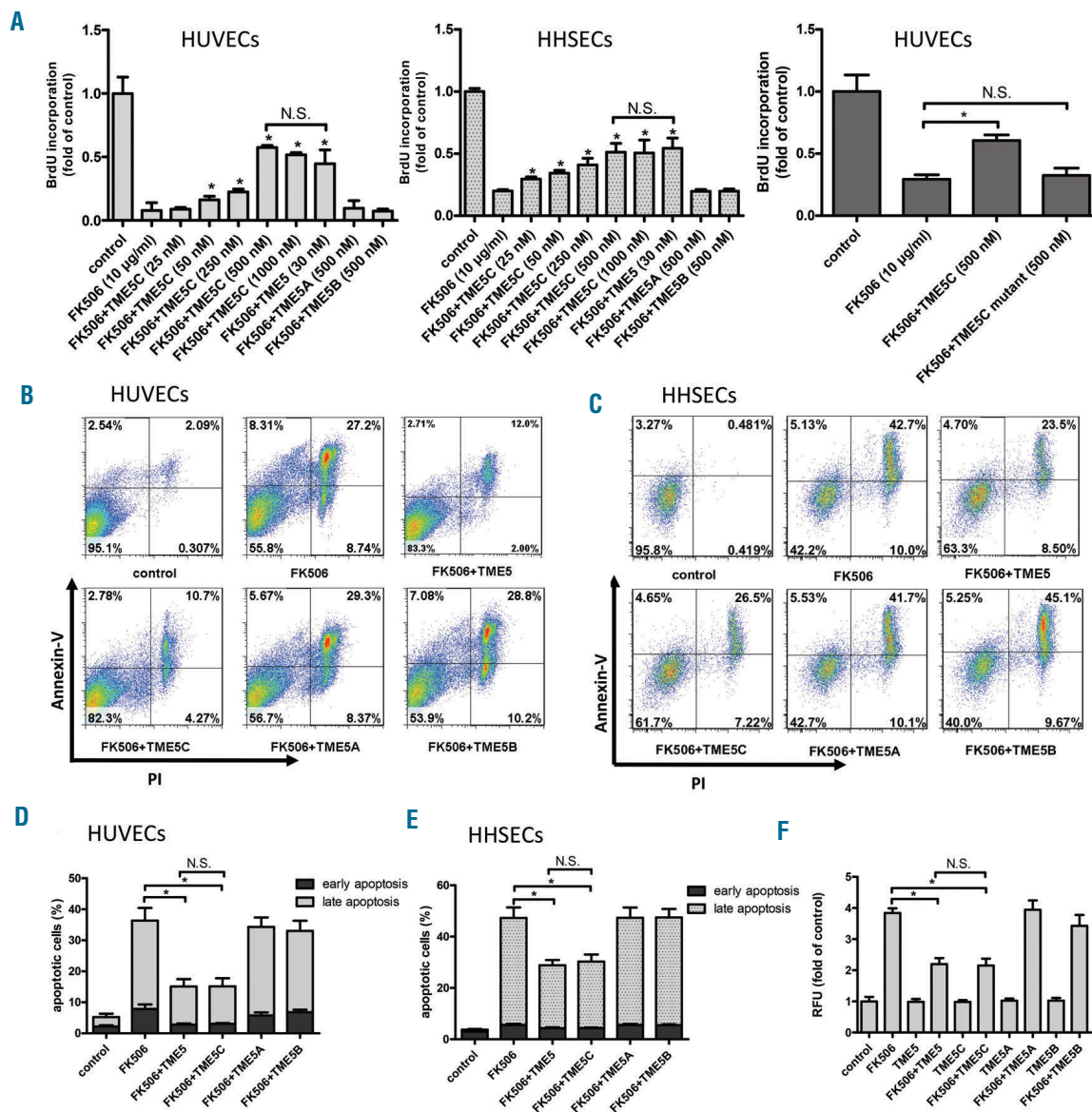


Figure 3. TME5C blocks apoptosis of FK506-treated endothelial cells. (A). BrdU incorporation assay. HUVECs or HHSECs were cultured with TME5C (25, 50, 250, 500, 1000 nM), TME5A (500 nM), TME5B (500 nM), TME5C mutant (500 nM), or TME5 (30 nM) in combination with FK506 (10 μ g/ml) for 24 h. Proliferation was measured by BrdU incorporation assays (n=3). (B, C). Apoptosis assays. HUVECs or HHSECs were exposed to FK506 (10 μ g/ml) with or without TME5A/B/C (500 nM) or TME5 (30 nM). After 36 h, cells were harvested, stained with anti-annexin V and PI, and subjected to FACS. Annexin V+PI- and Annexin V+PI+ indicate early and late apoptosis, respectively. (D, E). Quantitative analysis of the apoptotic cells in each group (n=3). (F). Vascular permeability assays. HUVEC monolayers were exposed to TME5 (30 nM) or TME5A/B/C (500 nM) with or without FK506 (10 μ g/ml) for 12 h, and then fluorescein isothiocyanate-dextran was added. The fluorescence of the plate well solution was measured to quantify the extent of permeability. Experiments were performed three times. Results represent the mean \pm SD. *P<0.05. BrdU: bromodeoxyuridine; HUVECs: human umbilical vein endothelial cells; HHSECs: human hepatic sinusoidal endothelial cells; PI: propidium iodide. FK506: tacrolimus; TM: thrombomodulin; N.S.: not significant.

between two groups under multiple conditions using one-way analysis of variance (ANOVA) followed by Bonferroni multiple comparison tests using GraphPad Software (La Jolla, CA, USA). Differences in animal survival (Kaplan-Meier survival curves) were analyzed by log-rank test. A P -value < 0.05 was considered statistically significant.

Results

TME5C, but not TME5A or TME5B, stimulates proliferation of endothelial cells

Figure 1A shows the amino acid sequences of TM mutants TME5A, TME5B, and TME5C. We first examined the effects of each TM mutant on the proliferation of

HUVECs or HHSECs. Exposure to TME5C (25-1000 nM) but not molar equivalents of TME5A or TME5B stimulated their proliferation in a dose-dependent manner, as assessed by BrdU incorporation assays. For example, 500 nM TME5C stimulated proliferation of HUVEC and HHSECs by nearly 1.5-fold. The highest dose of TME5C (1000 nM) did not further stimulate the proliferation of HUVECs and HHSECs (Figure 1B). TME5 also stimulated the proliferation of endothelial cells in a dose-dependent manner, which was consistent with our previous study.²⁵ TME5 produced the maximum pro-proliferative effect at a concentration of 30 nM (*Online Supplementary Figure S1*).

We conducted further experiments with a TME5C mutant with a single amino acid substitution (G→A, Table 1). This mutant form of TME5C lost the ability to

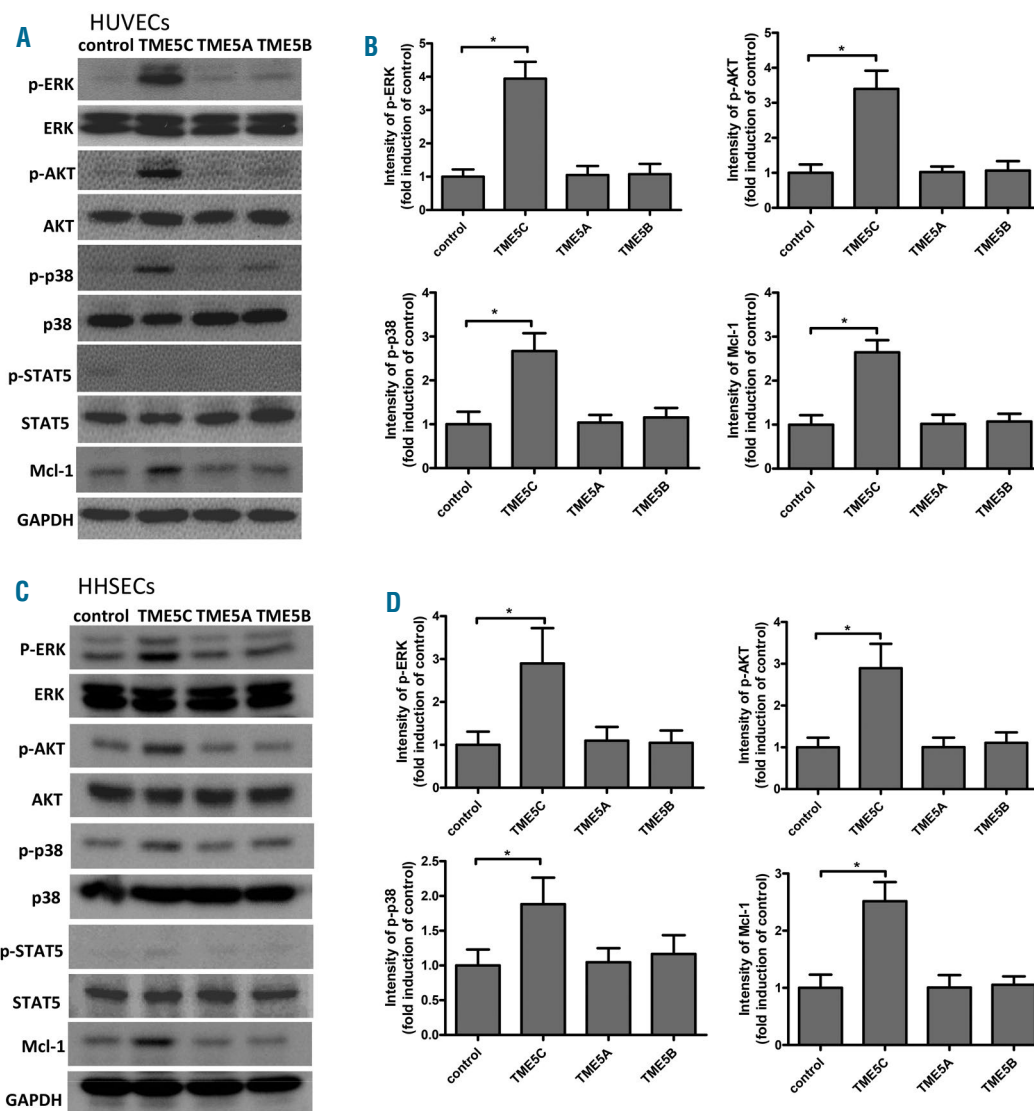


Figure 4. TME5C increases the levels of p-ERK, p-AKT, p-p38, and Mcl-1 in endothelial cells. (A and C). HUVECs or HHSECs were exposed to control diluents (PBS as control) or TM mutants (500 nM). After 48 h, proteins were extracted and subjected to western blot analyses. The membrane was sequentially probed with the indicated antibodies. (B and D). Relative quantifications of p-ERK, p-AKT, p-p38, and Mcl-1. ImageJ software was used to measure the band intensities after western blotting. All experiments were performed three times. Results represent the mean \pm SD. * $P < 0.05$. TM: thrombomodulin; HUVECs: human umbilical vein endothelial cells; HHSECs: human hepatic sinusoidal endothelial cells.

stimulate the proliferation of HUVECs, suggesting that the pro-proliferative effect of TME5C was dependent on the specific amino acid sequence of this peptide (Figure 1C).

TME5C stimulates angiogenesis

The potential role of TME5C to stimulate angiogenesis was examined *in vitro* and *in vivo*. TME5C (500 nM) but not TME5A or TME5B stimulated vascular tube formation of HUVECs and HHSECs by nearly 3-fold compared with control diluent-treated cells (Figure 2A-D). On the other hand, no remarkable proangiogenic effect was noted in the mutant form of TME5C (Figure 2E,F). Furthermore, *in vivo* angiogenesis assays with matrigel plugs revealed that TME5C (500 nM) stimulated angiogenesis in C57BL/6 mice (Figure 2G). In addition, the hemoglobin concentration was significantly increased in matrigel containing TME5C (Figure 2H) compared to matrigel containing control diluent. Consistent with the results of the proliferation assays, 30 nM TME5 produced an almost identical angiogenic effect with 500 nM TME5C (Figure 2A-D, G, H).

TME5C, but not TME5A or TME5B, blocks FK506-induced growth inhibition and apoptosis in endothelial cells

We examined whether TME5C counteracted the growth inhibition of HUVECs and HHSECs induced by the calcineurin inhibitor FK506. FK506 inhibited the proliferation of HUVECs and HHSECs by 80-90% and 70-80%, respectively. This growth inhibition was significantly attenuated by the presence of TME5C in a dose-dependent manner up to 500 nM (Figure 3A). The highest dose of TME5C (1000 nM) was not as potent as 500 nM TME5C. Neither TME5A (500 nM) nor TME5B (500 nM) counteracted the effect of FK506 on proliferation of HUVECs and HHSECs (Figure 3A). We therefore chose 500 nM of TME5C for subsequent experiments. Importantly, the mutant form of TME5C lost the ability to block FK506-induced growth inhibition (Figure 3A). We next examined whether TME5C could block FK506-induced apoptosis in HUVECs and HHSECs. FK506 induced more than 40% of HUVECs and HHSECs to be apoptotic. Interestingly, when these cells were cultured in the presence of both FK506 (10 $\mu\text{g}/\text{mL}$) and TME5C (500 nM), the population of apoptotic cells significantly

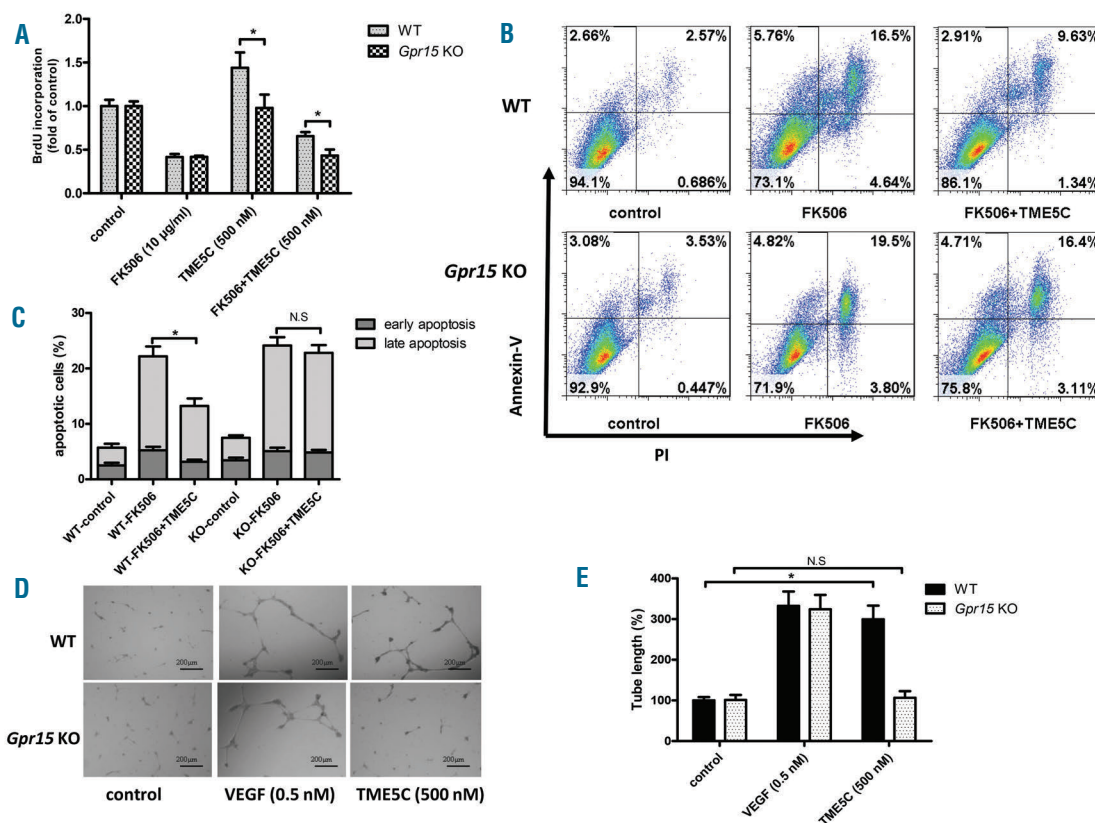


Figure 5. TME5C exerts cytoprotective function in murine ECs in a GPR15-dependent manner. (A). BrdU incorporation assays. WT or *Gpr15* KO murine ECs were cultured with TME5C (500 nM) with or without FK506 (10 $\mu\text{g}/\text{ml}$) for 24 h. Proliferation was measured by BrdU incorporation assays. (B). Apoptosis assay. WT or *Gpr15* KO murine ECs were exposed to FK506 (10 $\mu\text{g}/\text{ml}$) and/or TME5C (500 nM). After 36 h cells were harvested and stained with anti-annexin V and PI. FACS was used to analyze apoptotic cells. Annexin V+PI- and Annexin V+PI+ indicate early and late apoptosis, respectively. (C). Quantitative analysis of apoptotic cells in each group (n=3). (D, E). Vascular tube formation assays *in vitro*. WT or *Gpr15* KO murine ECs were plated on growth factor-reduced matrigel-precoated 24-well plates (2.0×10^4 cells/well) and incubated with control diluent, TME5C (500 nM), or VEGF (0.5 nM, positive control). After 8 h, the endothelial cell-derived tube-like structure was photographed using an inverted microscope. The tube length in three randomly chosen fields from each well was measured using NIH ImageJ software. Results represent the mean \pm SD. * $P < 0.05$. BrdU, bromodeoxyuridine; KO, knock out; GPR15: G-protein coupled receptor; WT: wild-type; FK506: tacrolimus; TM: thrombomodulin; N.S.: not significant; VEGF: vascular endothelial growth factor.

decreased (Figure 3B-E). By comparison, neither TME5A (500 nM) nor TME5B (500 nM) showed cytoprotective effects in HUVECs and HHSECs. In parallel with the induction of apoptosis, vascular permeability was profoundly induced in HUVECs after exposure to FK506 (10 µg/ml) for 12 h. Of note, FK506-induced vascular permeability was significantly attenuated in the presence of TME5C (500 nM), but not TME5A or TME5B (Figure 3F). Once more, a lower dose of TME5 (30 nM) produced a cytoprotective effect comparable to 500 nM TME5C (Figure 3).

TME5C upregulates p-ERK, p-AKT, p-p38, and Mcl-1 in endothelial cells

We examined whether TME5C acts through the intracellular signal transduction pathways in HUVECs and HHSECs. Western blot analysis with different antibodies against intracellular signal transduction pathways found that exposure of either HUVECs or HHSECs to TME5C (500 nM) but not TME5A (500 nM) or TME5B (500 nM) for 48 h significantly increased the levels of phospho (p)-ERK, p-AKT, p-p38, and Mcl-1 in these cells (Figure 4A-D).

GPR15 is indispensable for the effects of TME5C

Further experiments were carried out to test whether GPR15 also mediated the cytoprotective function of TME5C as it did for TME5. BrdU incorporation assays found that TME5C stimulated the proliferation of ECs isolated from WT C57BL/6 mice by nearly 1.5-fold compared with ECs treated with control diluent. In contrast, TME5C was not able to stimulate the proliferation of vascular ECs isolated from *Gpr15* KO mice (Figure 5A). In

addition, TME5C significantly rescued the ECs isolated from WT C57BL/6 mice, but not *Gpr15* KO mice, from FK506-induced growth inhibition and apoptosis (Figure 5A-C). Moreover, TME5C stimulated vascular tube formation in WT C57BL/6 murine ECs but not *Gpr15* KO murine ECs (Figure 5D,E).

TME5C does not affect thrombin-mediated coagulation

The fourth, fifth and sixth region of EGF-like domain of TM (TME456) binds thrombin and converts protein C to APC.³² The present study explored whether TME5C binds thrombin by measuring PT and APTT. rTM (500 nM) prolonged PT and APTT by approximately 200% and 165%, respectively. A much higher concentration of rTM (5000 nM) prolonged PT and APTT by more than 400% and 900%, respectively. Interestingly, TME5 (5000 nM) also prolonged PT and APTT by 137% and 225%, respectively. Of note, even the highest concentration of 5000 nM TME5C did not prolong either PT or APTT (Figure 6).

TME5C ameliorates SOS in a murine model

To induce SOS, we used a murine BMT model preconditioned with BU and CY (Figure 7A). BMT recipients treated with PBS showed a decrease in food intake, curled hairs, and abdominal distention (*data not shown*). Dark brown colored livers indicating congestion and massive ascites were noted in BMT recipients treated with PBS on day 7 after BMT (Figure 7B,C). In addition, liver enzymes, including ALT and AST, were significantly elevated in BMT recipients treated with PBS at day 7 (Figure 7D). On the other hand, these indicators were less significant in

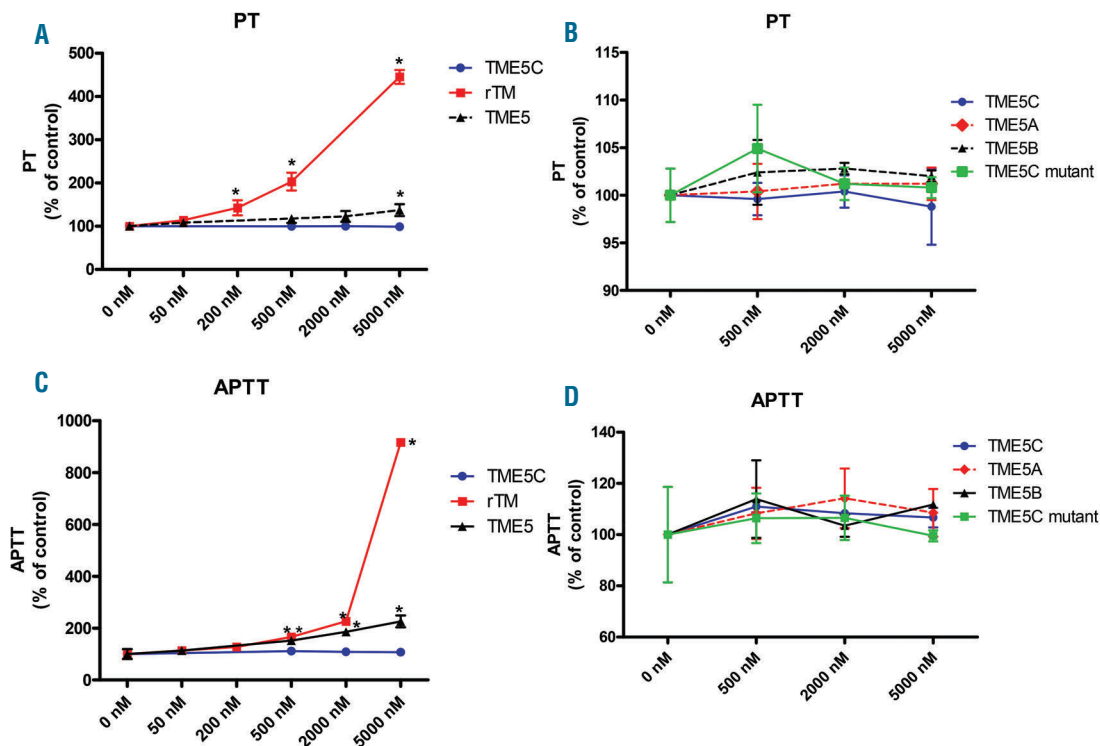


Figure 6. Effects of TME5C on PT and APTT. Plasma was obtained from a healthy volunteer and mixed with PT or APTT reagent with or without a series of TM fragments at various concentrations. (A, B). PT assays of TM fragments. (C, D). APTT assays of TM fragments. Experiments were performed three times. Results represent the mean \pm SD. * $P < 0.05$ compared with control. PT: prothrombin time; APTT: activated partial thromboplastin time; TM: thrombomodulin; rTM: recombinant human soluble thrombomodulin.

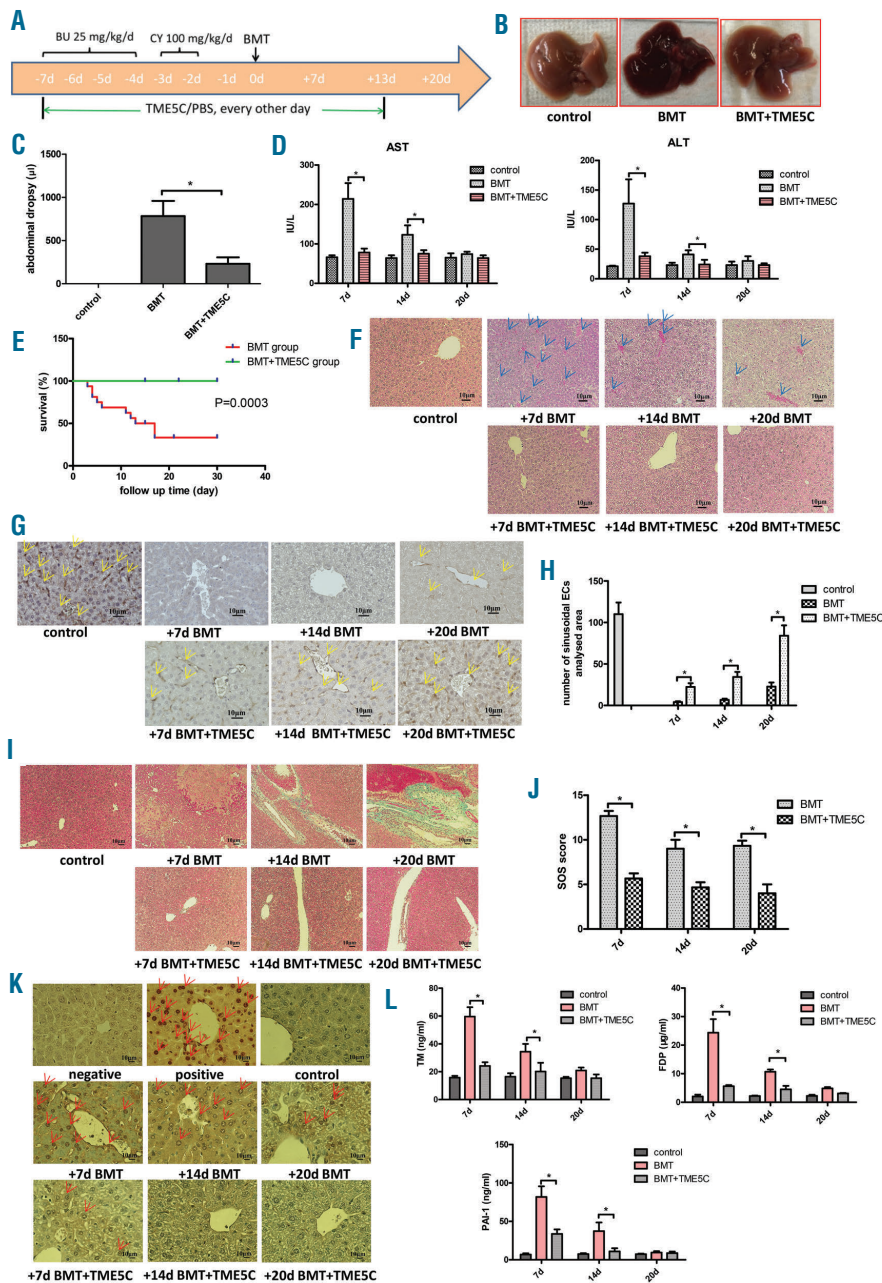


Figure 7. TME5C ameliorates SOS in mice. C57BL/6 mice were randomly divided into three groups (n=16 in each group): untreated mice without BMT were defined as the control group, BMT recipient mice treated with vehicle PBS were defined as the BMT group, and BMT recipient mice treated with TME5C were defined as the BMT+TME5C group. (A). Schematic diagram of SOS model with the schedule of treatment. (B). Liver macroscopic picture of mice. On day 7 after BMT, some mice were sacrificed, and their livers were photographed. The images show representative livers of mice in each group. (C). Volume of ascites. On day 7 after BMT, ascites was harvested from mice (n=3 per group) and weighed. (D). Plasma levels of liver enzymes. On days 7, 14, and 20 after BMT, blood was collected from mice (n=3 per group), and plasma levels of AST and ALT were measured. (E). Survival of mice. Survival of mice was monitored every day. (F, G, I). H&E, IHC, and Masson staining (H&E and Masson x100, IHC x200). On days 7, 14, and 20 after BMT, some mice were sacrificed. Livers were removed and fixed with formaldehyde solution for H&E staining (blue arrow shows necrosis of hepatocytes and obstruction of liver sinusoid). Some liver slices were incubated with primary pan-endothelial cell monoclonal antibody (MECA-32) for IHC staining. Yellow arrows indicate the sinusoidal ECs. Masson staining was also carried out to evaluate the sinusoidal fibrosis of liver. Blue indicates collagen. (H). Quantification of MECA-32 positive-stained sinusoidal ECs in each group (n=3 in each group). (J). SOS score. Scoring of light microscopy histological slices stained with H&E or Masson stain were blindly evaluated according to the scoring system. (K). TUNEL stain (x400). Apoptosis of hepatocytes were assessed using an *in situ* cell death detection kit. Red arrows indicate apoptotic hepatocytes and sinusoidal ECs. (L). ELISA. Plasma was collected for ELISA to measure the concentrations of TM, FDP, and PAI-1. Results represent the mean \pm SD. * $P < 0.05$. BU: busulfan; CY: cyclophosphamide; BMT: bone marrow transplantation; H&E, hematoxylin-eosin; IHC, immunohistochemistry; TM: thrombomodulin; FDP: fibrin degradation product; PAI-1: plasminogen activator inhibitor-1; PBS: phosphate buffered saline.

BMT recipients treated with TME5C (Figure 7B-D). Strikingly, 9 out of 16 (56.3%) BMT recipient mice treated with PBS died by day 30 after BMT (Figure 7E), while none of the BMT recipient mice treated with TME5C died during the experimental period (Figure 7E).

Pathological examination of livers removed from BMT mice treated with PBS on day 7 showed severe hemorrhagic necrosis with partial obstruction of liver sinusoids, infiltration of inflammatory cells, subendothelial hemorrhage, and loss of liver sinusoidal lining cells (Figure 7F). IHC staining of ECs with MECA-32 indicated a decrease in the number of sinusoid ECs, loss of integrity of sinusoid walls, and liver sinusoidal EC detachment (Figure 7G,H). These liver abnormalities were partly recovered by the 20th day after BMT in PBS-treated mice. In addition,

Masson staining demonstrated massive sinusoidal fibrosis with collagen deposition in livers removed from BMT recipients treated with PBS (Figure 7I). Importantly, all liver damage and associated findings were less severe in BMT recipients treated with TME5C. Careful pathological examination of livers with the SOS scoring system also found that the severity of SOS was significantly less in BMT recipients treated with TME5C than in those treated with PBS throughout the experimental period (Figure 7J). Moreover, TUNEL assays identified fewer apoptotic hepatocytes and sinusoid ECs in livers removed from TME5C-treated BMT mice compared with livers removed from BMT recipients treated with PBS (Figure 7K).

We additionally measured plasma levels of TM, FDP,

and PAI-1, which are recognized markers of endothelial cell damage and coagulopathy in these mice. All of these markers steeply increased in PBS-treated BMT mice at the 7th day after BMT. Levels of these markers were significantly lower in BMT recipients treated with TME5C than in those treated with PBS (Figure 7L).

Discussion

Our previous study found that the cytoprotective effects of TM were preserved in TME5.^{24,26} TME5 consists of three loops: A, B, and C (Figure 1A). The C-loop in the C-terminal subdomain is formed by a stretch of amino acids between the fifth and sixth cysteine residues, and its amino acid sequence is longer than those of the other two loops.²⁷ The C loop contains a short tri-stranded β -sheet structure,³³ and is more similar to EGF when compared to the A or B loops.²⁷ The study herein found that TME5C, but not A or B, exerted pro-angiogenic and cytoprotective effects in a GPR15-dependent manner both *in vitro* and *in vivo*. Strikingly, TME5C ameliorated HSCT-associated SOS in a murine model.

We previously showed that TME5 did not produce APC,²⁴ but retained some binding capacity towards thrombin (Figure 6). The present study found that TME5C lost the ability to interact with thrombin, as TME5C did not affect PT or APTT (Figure 6). The ratio of concentration of TME5 that affect cytoprotection (30 nM) to coagulation (5000 nM) was approximately 1:166. The concentration of TME5C that produced cytoprotection was 500 nM. However, even the 166-fold higher concentration of TME5C (83 μ M) did not prolong APTT (*data not shown*). Thus, the use of TME5C may be safe for BMT recipients as well as SOS patients who are at risk of bleeding due to low platelet counts and/or coagulopathy.

We have recently identified GPR15 as a binding partner of TME5 by performing a pull-down assay with membrane protein isolated from HUVECs followed by matrix assisted laser desorption ionization-time of flight mass spectrometry (MALDI-TOF MS) analysis.²⁵ We found that the cytoprotective and pro-angiogenic effects of TME5 were mediated by GPR15, as neither cytoprotection nor angiogenesis is noted in vascular endothelial cells isolated from *Gpr15* KO mice after exposure to TME5.²⁵ The study herein found that TME5C exerts cytoprotective and pro-angiogenic effects in vascular ECs isolated from wild-type C57BL/6 mice, but not in ECs isolated from *Gpr15* KO mice, suggesting that TME5C also produces favorable effects in ECs *via* GPR15.

GPR15 is also expressed on T lymphocytes and is required for infection of HIV as a co-receptor.³⁴ Accumulating evidence suggests the involvement of GPR15 in the regulation of inflammation; GPR15 expressed on murine TH1 and TH17 effector cells is

implicated in the development of colitis.³⁵ However, the expression of GPR15 on regulatory T cells is associated with the accumulation of these cells in the intestines and the alleviation of colitis.³⁶ GPR15 is also required for the homing of dendritic epidermal T cells into epidermal tissues.³⁴ Intriguingly, TME5 inhibits mixed lymphocyte reactions *in vitro* in association with a decrease in the production of inflammatory cytokines such as interleukin-6 and tumor necrosis factor α .³⁷ The anti-inflammatory effect of TME5 is also mediated by GPR15, as TME5 was not able to inhibit the mixed lymphocyte reaction when we used lymphocytes isolated from *Gpr15* KO mice.³⁷ Of note, the use of TME5 significantly alleviated graft-versus-host disease (GvHD) in a murine model.³⁷ TME5 also rescues mice from LPS-induced sepsis,²⁶ further confirming the anti-inflammatory function of TME5C.

Liver sinusoidal ECs are not only the supporting cells of quiescent hepatocytes, but also the source of vascularization during liver regeneration.³⁸ Hepatocytes undergo apoptosis in parallel with a decrease in vascularization when sinusoidal ECs are damaged.³¹ EC insults cause a hypercoagulable state through the upregulation of tissue factor and downregulation of TM on ECs, leading to the formation of fibrin clots in the microvasculature.³¹ As a consequence, the fibrinolytic system is activated to form various FDP fragments. Of note, PAI-1, an important antifibrinolytic regulator mainly produced by ECs, impedes fibrinolysis by inhibiting tissue plasminogen activator and augments thrombus formation.³⁹ Interestingly, the levels of PAI-1 are elevated in SOS patients but not in patients with GvHD and other liver injuries, suggesting that PAI-1 might be a marker capable of discriminating SOS from other BMT-related complications.⁴⁰ Increases in plasma levels of TM, FDP, and PAI-1 were noted in the murine SOS model, and they were significantly counteracted by the use of TME5C (Figure 7L), indicating cytoprotective roles of TME5C *in vivo*.

The optimum effective concentration of TME5C in our experiment (500 nM) was higher than that of TME5 (30 nM). TME5 was produced by the yeast *Pichia*, while TME5C is a chemically synthesized peptide, therefore we cannot precisely compare the potency of these two compounds. However, it is possible that the C-loop alone is not enough to fully produce the pro-proliferative and proangiogenic effect of TM.

Taken together, TME5C, which does not affect the coagulation system, exerts pro-angiogenic and cytoprotective activities both *in vitro* and *in vivo*. Hence, the use of TME5C may be a promising strategy to prevent and/or treat HSCT-related complications, including SOS.

Funding

This study was supported by Asahi Kasei Pharma (Tokyo, Japan), Uehara Memorial Foundation, and KAKENHI (26461406).

References

- Richardson PG, Ho VT, Cutler C, et al. Hepatic veno-occlusive disease after hematopoietic stem cell transplantation: novel insights to pathogenesis, current status of treatment, and future directions. *Biol Blood Marrow Transplant.* 2013;19(1 Suppl):S88-90.
- Mohty M, Malard F, Abecassis M, et al. Sinusoidal obstruction syndrome/veno-occlusive disease: current situation and perspectives—a position statement from the European Society for Blood and Marrow Transplantation (EBMT). *Bone Marrow Transplant.* 2015;50(6):781-789.
- Senzolo M, Germani G, Cholongitas E, et al. Venous occlusive disease: update on clinical management. *World J Gastroenterol.* 2007;13(29):3918-3924.
- Palomo M, Diaz-Ricart M, Carbo C, et al.

- Endothelial dysfunction after hematopoietic stem cell transplantation: role of the conditioning regimen and the type of transplantation. *Biol Blood Marrow Transplant.* 2010;16(7):985-993.
5. Vion AC, Rautou PE, Durand F, et al. Interplay of inflammation and endothelial dysfunction in bone marrow transplantation: focus on hepatic veno-occlusive disease. *Semin Thromb Hemost.* 2015; 41(6):629-643.
 6. Carreras E, Diaz-Ricart M. The role of the endothelium in the short-term complications of hematopoietic SCT. *Bone Marrow Transplant.* 2011;46(12):1495-1502.
 7. Tuncer HH, Rana N, Milani C, et al. Gastrointestinal and hepatic complications of hematopoietic stem cell transplantation. *World J Gastroenterol.* 2012;18(16):1851-1860.
 8. Bearman SI, Lee JL, Baron AE, et al. Treatment of hepatic veno-occlusive disease with recombinant human tissue plasminogen activator and heparin in 42 marrow transplant patients. *Blood.* 1997;89(5):1501-1506.
 9. Haussmann U, Fischer J, Eber S, et al. Hepatic veno-occlusive disease in pediatric stem cell transplantation: impact of pre-emptive antithrombin III replacement and combined antithrombin III/defibrotide therapy. *Haematologica.* 2006;91(6):795-800.
 10. Bearman SI, Shen DD, Hinds MS, et al. A phase I/II study of prostaglandin E1 for the prevention of hepatic veno-occlusive disease after bone marrow transplantation. *Br J Haematol.* 1993;84(4):724-730.
 11. Esmon CT, Esmon NL, Harris KW. Complex formation between thrombin and thrombomodulin inhibits both thrombin-catalyzed fibrin formation and factor V activation. *J Biol Chem.* 1982;257(14):7944-7947.
 12. O'Brien LM, Mastro M, Fay PJ. Regulation of factor VIIIa by human activated protein C and protein S: inactivation of cofactor in the intrinsic factor Xase. *Blood.* 2000; 95(5):1714-1720.
 13. Kalafatis M, Rand MD, Mann KG. The mechanism of inactivation of human factor V and human factor Va by activated protein C. *J Biol Chem.* 1994;269(50):31869-31880.
 14. Dahlback B, Villoutreix BO. The anticoagulant protein C pathway. *FEBS Lett.* 2005; 579(15):3310-3316.
 15. Schuepbach RA, Madon J, Ender M, et al. Protease-activated receptor-1 cleaved at R46 mediates cytoprotective effects. *J Thromb Haemost.* 2012;10(8):1675-1684.
 16. Ikezoe T, Takeuchi A, Taniguchi A, et al. Recombinant human soluble thrombomodulin counteracts capillary leakage associated with engraftment syndrome. *Bone Marrow Transplant.* 2011;46(4):616-618.
 17. Ikezoe T, Togitani K, Komatsu N, et al. Successful treatment of sinusoidal obstructive syndrome after hematopoietic stem cell transplantation with recombinant human soluble thrombomodulin. *Bone Marrow Transplant.* 2010;45(4):783-785.
 18. Nakamura D, Yoshimitsu M, Kawada H, et al. Recombinant human soluble thrombomodulin for the treatment of hepatic sinusoidal obstructive syndrome post allogeneic hematopoietic SCT. *Bone Marrow Transplant.* 2012;47(3):463-464.
 19. Ohwada C, Takeuchi M, Kawaguchi T, et al. Successful treatment with recombinant soluble thrombomodulin of two cases of sinusoidal obstructive syndrome/hepatic veno-occlusive disease after bone marrow transplantation. *Am J Hematol.* 2011; 86(10):886-888.
 20. Yamamoto S, Yagawa A, Toyama D, et al. Successful treatment of hepatic sinusoidal obstructive syndrome after hematopoietic stem cell transplantation in a child using recombinant thrombomodulin. *Acta Haematol.* 2013;129(1):62-64.
 21. Fujiwara H, Maeda Y, Sando Y, et al. Treatment of thrombotic microangiopathy after hematopoietic stem cell transplantation with recombinant human soluble thrombomodulin. *Transfusion.* 2016;56(4): 886-892.
 22. Ikezoe T, Yang J, Nishioka C, et al. Thrombomodulin protects endothelial cells from a calcineurin inhibitor-induced cytotoxicity by upregulation of extracellular signal-regulated kinase/myeloid leukemia cell-1 signaling. *Arterioscler Thromb Vasc Biol.* 2012;32(9):2259-2270.
 23. Ikezoe T, Yang J, Nishioka C, et al. Thrombomodulin blocks calcineurin inhibitor-induced vascular permeability via inhibition of Src/VE-cadherin axis. *Bone Marrow Transplant.* 2017;52(2):245-251.
 24. Ikezoe T, Yang J, Nishioka C, et al. The fifth epidermal growth factor-like region of thrombomodulin exerts cytoprotective function and prevents SOS in a murine model. *Bone Marrow Transplant.* 2017;52(1):73-79.
 25. Pan B, Wang X, Nishioka C, et al. G-protein coupled receptor 15 mediates angiogenesis and cytoprotective function of thrombomodulin. *Sci Rep.* 2017;7(1):692.
 26. Pan B, Wang X, Kojima S, et al. The fifth epidermal growth factor like region of thrombomodulin alleviates LPS-induced sepsis through interacting with GPR15. *Thromb Haemost.* 2017;117(3):570-579.
 27. Sampoli Benitez BA, Hunter MJ, Meininger DP, et al. Structure of the fifth EGF-like domain of thrombomodulin: An EGF-like domain with a novel disulfide-bonding pattern. *J Mol Biol.* 1997;273(4):913-926.
 28. Kobayashi M, Inoue K, Warabi E, et al. A simple method of isolating mouse aortic endothelial cells. *J Atheroscler Thromb.* 2005;12(3):138-142.
 29. Qiao J, Fu J, Fang T, et al. Evaluation of the effects of preconditioning regimens on hepatic veno-occlusive disease in mice after hematopoietic stem cell transplantation. *Exp Mol Pathol.* 2015;98(1):73-78.
 30. DeLeve LD, McCuskey RS, Wang X, et al. Characterization of a reproducible rat model of hepatic veno-occlusive disease. *Hepatology.* 1999;29(6):1779-1791.
 31. Zeng L, An L, Fang T, et al. A murine model of hepatic veno-occlusive disease induced by allogeneic hematopoietic stem cell transplantation. *Cell Biochem Biophys.* 2013;67(3):939-948.
 32. Stearns DJ, Kurosawa S, Esmon CT. Microthrombomodulin. Residues 310-486 from the epidermal growth factor precursor homology domain of thrombomodulin will accelerate protein C activation. *J Biol Chem.* 1989;264(6):3352-3356.
 33. Tejero R, Bassolino-Klimas D, Bruccoleri RE, et al. Simulated annealing with restrained molecular dynamics using CONGEN: energy refinement of the NMR solution structures of epidermal and type-alpha transforming growth factors. *Protein Sci.* 1996;5(4):578-592.
 34. Lahl K, Sweere J, Pan J, et al. Orphan chemoattractant receptor GPR15 mediates dendritic epidermal T-cell recruitment to the skin. *Eur J Immunol.* 2014;44(9):2577-2581.
 35. Nguyen LP, Pan J, Dinh TT, et al. Role and species-specific expression of colon T cell homing receptor GPR15 in colitis. *Nat Immunol.* 2015;16(2):207-213.
 36. Kim SV, Xiang WV, Kwak C, et al. GPR15-mediated homing controls immune homeostasis in the large intestine mucosa. *Science.* 2013;340(6139):1456-1459.
 37. Pan B, Wang X, Kojima S, et al. The fifth epidermal growth factor-like region of thrombomodulin alleviates murine graft-versus-host disease in a G-protein coupled receptor 15 dependent manner. *Biol Blood Marrow Transplant.* 2017; 23(5):746-756.
 38. el Mouelhi M, Kauffman FC. Sublobular distribution of transferases and hydrolases associated with glucuronide, sulfate and glutathione conjugation in human liver. *Hepatology.* 1986;6(3):450-456.
 39. Park YD, Yasui M, Yoshimoto T, et al. Changes in hemostatic parameters in hepatic veno-occlusive disease following bone marrow transplantation. *Bone Marrow Transplant.* 1997;19(9):915-920.
 40. Salat C, Holler E, Kolb HJ, et al. Plasminogen activator inhibitor-1 confirms the diagnosis of hepatic veno-occlusive disease in patients with hyperbilirubinemia after bone marrow transplantation. *Blood.* 1997;89(6):2184-2188.